Experiment and analysis of the effect of fine tracking system on the unstable platform in laser communication*

DONG Ran (董冉)**, **AI Yong** (艾勇), **XIONG Zhun** (熊准), **and SHAN Xin** (单欣)
School of Electronic Information, Wuhan University, Wuhan 430079, China

(Received 11 February 2013)

Atmospheric turbulence and platform vibration in the space optical communication can cause the offset and jitter of beam, which further result in the fluctuations of received optical power. To resist this effect, a communication system with fine tracking systems in the receiver and transmitter is designed. The system is used in the experiment of laser communication between high-rise buildings over a distance of 3.5 km. After adding a vibration source to the transmitter, the centroids of spots captured by the camera of the transmitter and the optical power of receiver are recorded for the purpose of analysis. When the vibration source works at the designated frequency, a peak appears at the corresponding frequency in the spectrum of the spot centroids and the optical power of receiver. Then the peak disappears once the fine tracking system begins to work. Compared with the condition without the fine tracking system, the minimum value of the optical power of receiver is increased by 5 dB, and the standard deviation is decreased by 30%.
Document code: A **Article ID:** 1673-1905(2013)04-0301-4
DOI 10.1007/s11801-013-3006-6

In recent years, the space laser communication becomes a hot research topic due to its excellent confidentiality, high communication speed, light-weight communication port and other advantages, so some relevant technologies have taken a big leap forward[1,2]. The biggest difference between laser communication and microwave communication is that the former uses a much smaller divergence angle, which leads to higher energy utilization rate and confidentiality but requires accurate acquisition, pointing and tracking (APT) of beam. The turbulence of atmospheric channel can cause coupling loss to arise from angle-of-arrival fluctuation, while the vibration of platform of transmitter is also able to deflect the laser beam, producing pointing loss[3]. However, although there are many theoretical researches[4,5] at home and abroad regarding the change of optical power and bit error rate (BER) caused by platform vibration, most of them haven't taken the influence of atmospheric turbulence into consideration. In the commonly used compound-axis APT system[6], as regards the transmitter, the offset of the beacon beam, which is detected by the fine tracking unit and used as the basis of pointing, is caused by the platform vibration, the angle-of-arrival fluctuation from atmospheric turbulence and the residual error of coarse tracking. For the receiver, the optical signal received by the receiver is also influenced by the pointing offset and angle-of-arrival fluctuation and intensity fluctuation arising from atmospheric turbulence. Besides, the turbulence itself can also impact the precision of fine tracking system[7,8]. This paper introduces a personal computer (PC)-based fine tracking system, which is installed in the receiver and transmitter of the space optical communication in order to conduct a laser communication experiment between urban high-rise buildings over a distance of 3.5 km under the circumstance of adding vibration source to the transmitter.

The whole experiment system consists of the transmitter and receiver as shown in Fig.1. In the optical path, there is a telescope and a prism in front of the camera of the fine tracking system, whose total focal length is 5 m and pixel size is 10 μm. So, when the size of region of interest (ROI) of the camera is 256 × 256 pixels, the field of view (FOV) of the fine tracking system is calculated as 500 μrad.

The fine tracking system can be divided into three parts from the perspective of hardware, which are the detection module, control module and execution module. The parameters of the fine tracking system are shown in Tab.1. The detection module uses an MV-D1024E-160 camera of PhotonFocus. The control module consists of a PC, an image acquisition card and a digital to analog (D/A) card, while the execution module is a finite state machine (FSM)-300 voice coil motor-driven galvanometer. The received beam from the telescope focuses on the photo-surface of the camera, and the camera transfers the image data collected by the PC. After the data is processed, the PC directs the D/A card to produce corresponding analog voltage to drive the FSM. Then the offset of spot is compensated, and the beam is stabilized.

* This work has been supported by the Natural Science of Hubei Province in China (No.2010CDB08502).
** E-mail: dr1931@aliyun.com

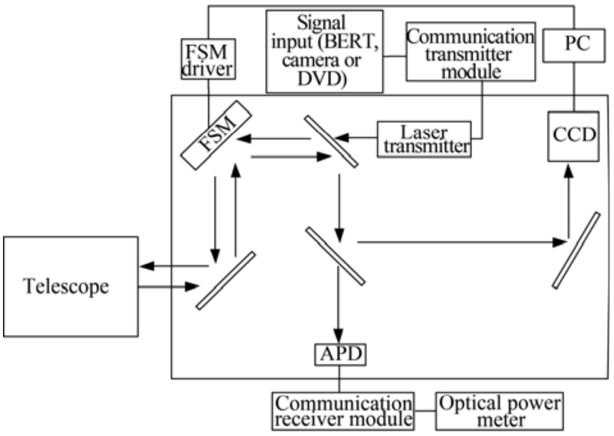

Fig.1 Block diagram of the experiment system

Tab.1 Parameters of the fine tracking system

Name	Major parameters
Sensor	MV-D1024E-160 camera; Resolution: 256×256, Frame frequency: 2200 f/s, FOV: 500 μrad
Control module	MicroEnable IV image acquisition card, PC, 12 bit AC6631 D/A card; Voltage setup time: ≤100 μs, Linearity :1 LSB (least-significant bit)
Execution module	FSM-300 FSM; Angular range: ±26.2 mrad（±1.5°）, Resolution: ≤1 μrad

A fine tracking software is programmed in C++ for the overall control of the system. It is mainly used for three purposes as follows: controlling the camera to adjust the exposure value and ROI, processing the image data and calculating spot centroids, calculating the voltage and outputting it by the D/A card.

The small FOV of the fine tracking system and short exposure time (less than 400 μs) both make the background of image quite simple. In addition, decreasing the operation time is helpful for the expansion of the bandwidth of fine tracking system. Therefore, an algorithm as fast as possible is used in the software.

The program starts to scan over the 1024×1024 pixels of full image to find the laser spot. Then the software adjusts the exposure time according to the strength of the light spot in the image to avoid over exposure and to improve location accuracy[9]. Then the Otsu algorithm is used to calculate the threshold, which is used as a fixed value to shorten the time of frame processing. After the threshold segmentation, the calculated spot centroid is used as the center of the ROI. In the last step, an incremental PID algorithm is used for calculating tracking control voltage to adapt to the wideband spot jitter caused by the turbulence and vibration[10]. The voltage $V(n)$ is computed according to

$$V(n)=V(n-1)+K_{\mathrm{P}}e(n)+K_{\mathrm{I}}\sum_{1}^{n}e(i)+ K_{\mathrm{D}}[e(n)-e(n-1)], \quad (1)$$

where $e(n)$ is the corresponding difference between the current spot centroid and the designated position.

The experimental laser communication link was established between the 18th floor of the teaching building in Wuhan University where the receiver was located and the 27th floor of a high-rise apartment building 3.6 km away from the transmitter. A beacon beam was transmitted from the receiver to the transmitter, and a signal beam was transmitted from the transmitter to the receiver. Because there was no feedback signal between the optical power meter and the fine tracking system, the manual pre-calibration was necessary. The received optical power was recorded at a sampling frequency of 10000 Hz at the receiver. The vibration source and the fine tracking system in transmitter were both switched between two states of ON and OFF. The laser spot centroids at the transmitter and the optical power of the receiver were recorded for analysis.

The data of coordinates of beacon spot centroid at the transmitter in different cases are shown in Fig.2 and Tab.2.

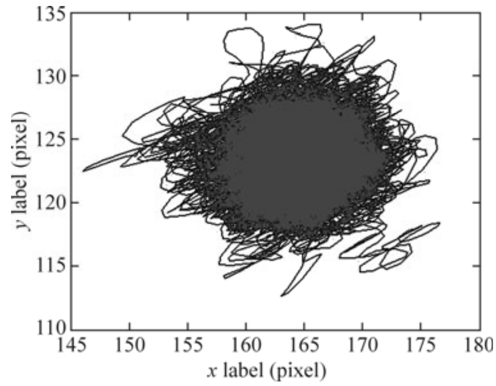

(a) Vibration OFF and tracking OFF

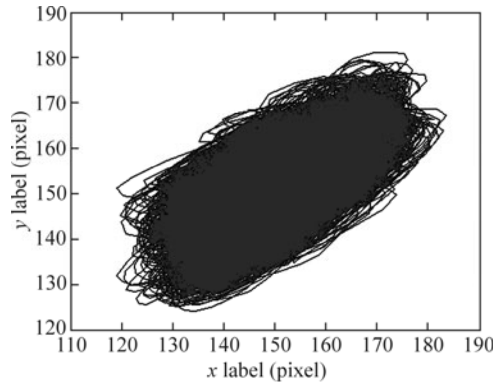

(b) Vibration ON and tracking OFF

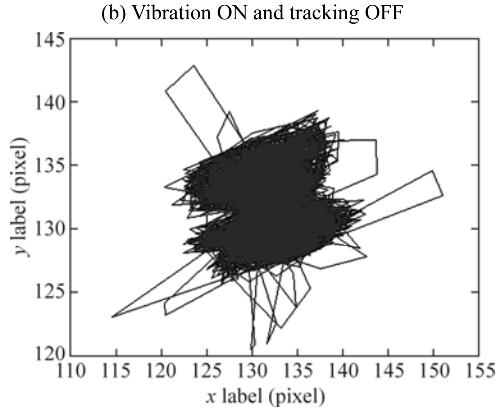

(c) Vibration ON and tracking ON

Fig.2 Distributions of centroids in different conditions

Tab.2 Statistical data of centroids' coordinates (STD: standard deviation; Avg: average)

	Vibration OFF and tracking OFF	Vibration ON and tracking OFF	Vibration OFF and tracking ON	Vibration ON and tracking ON
STD in *x*-axis (pixel)	3.36	11.80	10.66	5.59
STD in *y*-axis (pixel)	2.51	11.10	9.58	3.99
Max in *x*-axis (pixel)	176.60	182.00	183.30	148.00
Min in *x*-axis (pixel)	146.00	121.20	118.80	116.00
Avg in *x*-axis (pixel)	164.30	150.60	150.90	132.00
Max in *y*-axis (pixel)	134.00	181.40	181.00	145.80
Min in *y*-axis (pixel)	112.60	123.40	124.20	120.60
Avg in *y*-axis (pixel)	123.20	151.50	152.10	132.00

Fig.3 shows the frequency spectra of the spot centroids at the transmitter under different circumstances. As shown in Fig.3(b), a local peak of amplitude appears in the frequency spectrum at the frequency of 20 Hz due to the weak vibration source. And in Fig.3(c), the local peak of amplitude is at the frequency of 25 Hz, as twice of that in Fig.3(b). No matter in state of "vibration weak" or "vibration strong", the peak value at corresponding frequency appears, and the amplitudes at low frequencies (0–25 Hz) increase in a certain degree. Compared with Fig.3(c), it could be found in Fig.3(d) that the peak value at 25 Hz decreases significantly from 7.2 pixels to 1.6 pixels, and the amplitudes at low frequencies reduce too, but still fiercer than that under the "vibration OFF and tracking OFF" state.

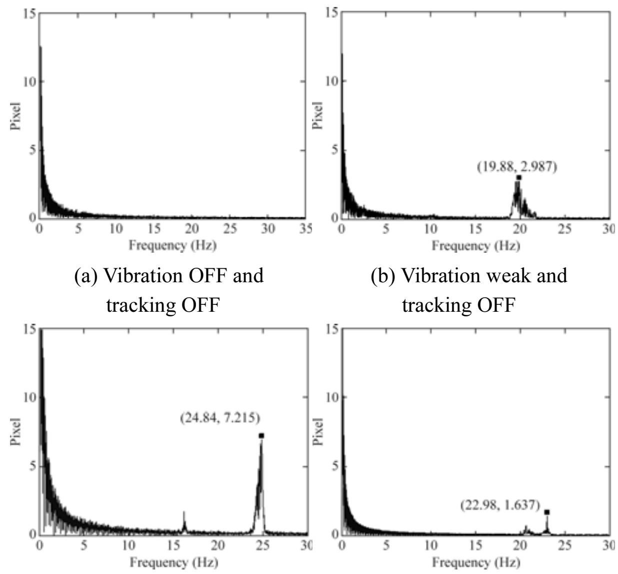

(a) Vibration OFF and tracking OFF (b) Vibration weak and tracking OFF

(c) Vibration strong and tracking OFF (d) Vibration strong and tracking ON

Fig.3 Frequency spectra of the spot centroids at the transmitter under different circumstances

The data recorded at the transmitter show that the operation of the vibration generator not only creates a peak at the corresponding frequency, but also enhances the spot jitter in a wideband. The fine tracking system of the transmitter mentioned in this paper can restrain the vibration significantly to reduce the pointing loss of the opposite receiver end and the coupling loss of the transmitter[11,12]. Because no optical power meter is installed in the transmitter, the changes of received optical power can not be recorded directly.

The frequency spectra and the statistical data of optical power at the receiver are shown in Fig.4 and Tab.3.

Comparing Fig.4(a) with (b), it can be found that when the transmitter is at the "vibration weak" state, the frequency spectrum of received optical power is much the same with that at the "vibration OFF" state, and only a few components at low frequencies (about below 50 Hz) increase. By comparing Fig.4(c) with (a), it is obvious that at the "vibration strong", not only all the amplitudes at all frequencies increase, but also the vibration source creates a corresponding peak value at the corresponding frequency of 25 Hz. Compared with Fig.4(c), Fig.4(d) shows that at the "tracking ON" state, the peak value at the frequency of 25 Hz disappears, but the overall amplitude still remains higher than that at the state of "vibration OFF".

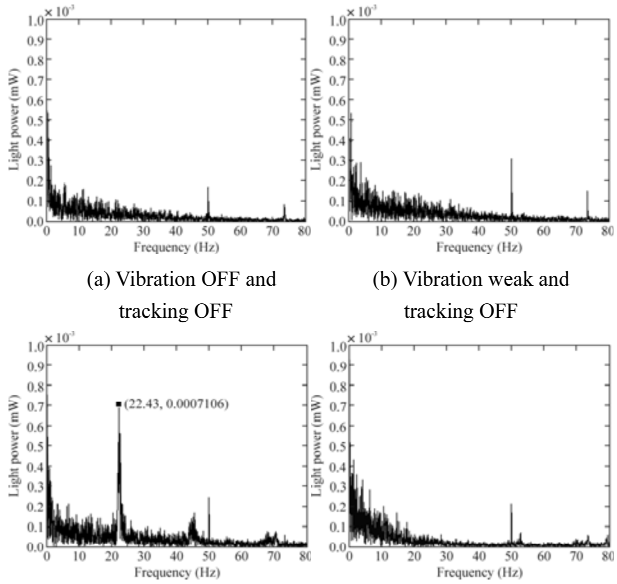

(a) Vibration OFF and tracking OFF (b) Vibration weak and tracking OFF

(c) Vibration strong and tracking OFF (d) Vibration strong and tracking ON

Fig.4 Frequency spectra of the optical power at the receiver under different circumstances

The statistic data shown in Tab.3 indicate that the vibration at the transmitter causes the increase of STD of received optical power. But the average optical power increases in some degree, which might result from the misalignment between transmitter's original direction and receiving end according to the analysis of project team. When the fine tracking system starts to work, the STD of optical power can be decreased, which is lower than that at “vibration ON and tracking OFF” state, but higher than that at “vibration OFF” state. The average value of optical power has a dramatic increase at the “tracking ON” state, which is the result of the fine tracking system correcting the location of transmitted signal beam.

Tab.3 Statistical data of the received optical power

	Vibration OFF and tracking OFF	Vibration strong and tracking OFF	Vibration weak and tracking OFF	Vibration strong and tracking ON
STD (μW)	1.354	2.222	1.789	1.720
Maximum (μW)	17.970	22.422	20.950	19.290
Minimum (μW)	2.230	1.449	1.242	3.792
Average (μW)	6.899	7.883	6.590	9.234

The conclusions are drawn via the analysis of data as follows. Firstly, in a free space optical communication system, if there is a strong vibration in one of the ends, frequency jitter will be produced in the beam spot of the end, as a result of which, the fiber coupling efficiency of this end will be greatly affected. At the same time, the jitter of laser beam transmitted by this end will be intensified, which leads to the fluctuation of the received optical power and the pointing loss of the opposite end. If there is a weak vibration in one of the ends, the impact on the received optical power of the opposite end can be buried in the fluctuation caused by the atmosphere turbulence. Secondly, in this experiment, the fine tracking system designed in this paper is installed in the same end with the vibration source. The vibration source creates a pulse in the spot jitter frequency spectrum as a peak of amplitude at the corresponding frequency. The fine tracking system can restrain the peak significantly, and weaken the wideband spot jitter caused by atmosphere turbulence. At the same time, the fluctuation of the received optical power of the opposite end is restrained too, and the minimum and average values of the optical power are increased.

Through this experiment, some aspects are required to be improved in the future. Due to the constraint of laboratory's condition, the influence of vibration source on the coupling efficiency of adjacent end is not measured directly, and its influence on the fine tracking system in the opposite end is not assessed, either. The frequency and amplitude of the vibration source used in the experiment can not be adjusted continuously. When the amplitude changes linearly, further researches are needed on the relationships between vibration amplitude and the coupling efficiency in the same end, and between vibration amplitude and the received optical power in the opposite end.

References

[1] Jiang Huilin, Hu Yuan, Ding Ying, Fu Dong, Keyan Song, Yansong Qiang, Zhao Yiwu and Lou Yan, Acta Optical Sinica **10**, 48 (2012). (in Chinese)

[2] FU Xing-hu, CHEN Zhen-yi, GUO Qiang, PANG Fu-fei, LI Ying-chun, SONG Ying-xiong and WANG Ting-yun, Journal of Optoelectronics·Laser **21**, 1013 (2010). (in Chinese)

[3] Tan Liying, Xie Wanqing, Ma Jing, Yang Yuqiang and Liu Qingfeng, High Power Laser and Partivle Beams **5**, 1193 (2011). (in Chinese)

[4] FU Qiang, JIANG Hui-lin, WANG Xiao-man, LIU Zhi, TONG Shou-feng and ZHANG Li-zhong, Chinese Optics **5**, 116 (2012). (in Chinese)

[5] WANG Jun, TIAN Bin and YI Ke-chu, Journal of Optoelectronics·Laser **21**, 551 (2010). (in Chinese)

[6] Huang Haibo, Zuo Tao, Chen Jing and Wang Weihua, Infrared and Laser Engineering **41**, 1561 (2012). (in Chinese)

[7] MA Jing, TAN Li-ying, JIN En-pei and Geng Wan-zheng, Journal of Astronautics **20**, 78 (1999). (in Chinese)

[8] Tao Zuo, Optoelectronics Letters **6**, 458 (2010).

[9] YU Si-yuan, TAN Li-ying, MA Jing and WANG Jun, Journal of Optoelectronics·Laser **15**, 472 (2004). (in Chinese)

[10] HAN Cheng, BAI Bao-xing, YANG Hua-ming and TONG Shou-feng, Acta Photonic Sinica **39**, 89 (2010). (in Chinese)

[11] LU Hong-qiang, ZHAO Wei and HU Hui, High Power Laser and Particle Beams **23**, 895 (2011). (in Chinese)

[12] Morio Toyoshima, J. Opt. Soc. Am. A **23**, 2246 (2006).